



# The effect of ciprofloxacin on doxorubicin cytotoxic activity in the acquired resistance to doxorubicin in DU145 prostate carcinoma cells

Asieh Davary Avareshk<sup>1</sup> · Razieh Jalal<sup>1,2</sup> · Jamileh Gholami<sup>1</sup>

Received: 17 March 2022 / Accepted: 28 June 2022

© The Author(s), under exclusive licence to Springer Science+Business Media, LLC, part of Springer Nature 2022

## Abstract

The present study aimed to assess the influence of ciprofloxacin (CIP) against the doxorubicin (DOX)-resistant androgen-independent prostate cancer DU145 cells. The DOX-resistant DU145 (DU145/DOX20) cells were established by exposing DU145 cells to the increasing concentrations of DOX. The antiproliferative effect of CIP was examined through employing MTT, colony formation, and 3D culture assays. DU145/DOX20 cells exhibited a twofold higher IC<sub>50</sub> value for DOX, an increased ABCB1 transporter activity, and some morphological changes accompanied by a decrease in spheroid size, adhesive and migration potential compared to DU145 cells. CIP (5 and 25 µg mL<sup>-1</sup>) resulted in a higher reduction in the viability of DU145/DOX20 cells than in DU145 cells. DU145/DOX20 cells were more resistant to CIP in 3D culture compared to the 2D one. No spheroid formation was observed for DU145/DOX20 cells treated with DOX and CIP combination. CIP and DOX, alone or in combination, significantly reduced the growth of DU145 spheroids. CIP in combination with 20 nM DOX prevented the colony formation of DU145 cells. The clonogenicity of DU145/DOX20 cells could not be estimated due to their low adhesive potential. CIP alone caused a significant reduction in the migration of DU145 cells and resulted in a more severe decrease in the wound closure ability of DOX-exposed ones. We identified that CIP enhanced DOX sensitivity in DU145 and DU145/DOX20 cells. This study suggested the co-delivery of low concentrations of CIP and DOX may be a promising strategy in treating the DOX-resistant and -sensitive hormone-refractory prostate cancer.

**Keywords** Ciprofloxacin · Clonogenicity · Doxorubicin-resistant cells · Migration ability · Prostate cancer · Spheroid growth

## Introduction

Doxorubicin (DOX), a member of anthracycline family, has been utilized as an agent to treat hormone-refractory prostate cancer (HRPC) [1] although its use is limited by its side effects and acquired resistance, which is a major clinical obstacle to successful treatment [2, 3]. DOX induces DNA

intercalation, DNA breaks, topoisomerase II inhibition, and free radical generation [4]. The mechanisms for drug resistance are complex, including increased drug efflux, decreased drug influx, drug target alternation, drug inactivation, enhanced DNA damage repair, and reduced apoptosis [5], all of which are energy-dependent and require ATP. Based on the results of in vitro studies, the drug-resistant cancer cells have higher intracellular ATP than the non-resistant ones do [6]. Emerging studies demonstrated that the growth of cancer cells declines when blocking major ATP-generating pathways, glycolysis and oxidative phosphorylation [6, 7].

The ciprofloxacin (CIP) belonging to fluoroquinolone family inhibits bacterial DNA topoisomerase II (DNA gyrase) [8] and has been commonly consumed for urinary tract and prostatic infections due to its ability to excrete and penetrate into urine and prostatic compartments perfectly [9]. Further, CIP inhibits eukaryotic topoisomerase II, especially its mitochondrial isoform, and eventually decreases

---

Asieh Davary Avareshk and Jamileh Gholami have contributed equally to this work.

✉ Razieh Jalal  
razieh@um.ac.ir

<sup>1</sup> Department of Chemistry, Faculty of Science, Ferdowsi University of Mashhad, Mashhad, Iran

<sup>2</sup> Novel Diagnostics and Therapeutics Research Group, Institute of Biotechnology, Ferdowsi University of Mashhad, Mashhad, Iran

mtDNA content and ATP production, and induces oxidative stress and intrinsic apoptotic pathway [10–12]. Several studies reported the safety and therapeutic efficacy of CIP and its combination with chemotherapeutic drugs on various cancer cells [13–16]. However, *in vitro* evidence have shown that CIP at high concentration exhibits anticancer activity. On the other hand, there are few reports on the ability of CIP to sensitize chemoresistant cancer cells to chemotherapeutic drugs, such as DOX and docetaxel [17–19].

To date, no study has focused on the effect of CIP on the DOX-resistant HRPC cells, to the best of our knowledge. In the present study, human prostate cancer DU145 cell line was used as a model of the androgen-independent prostate cancer cells and the DOX-resistant DU145 (DU1454/DOX20) subline was established by continuous exposure to the increasing concentrations of DOX. Then, the effect of CIP was evaluated on the cell proliferation, migration, colony, and spheroid formation of DU145 and DU145/DOX20 cells. Moreover, the ABCB1 function and the mRNA expression of ABCB4 were assessed using efflux transporter activity assays and qRT-PCR, respectively. Low concentrations of CIP seem to improve the anticancer efficacy of DOX on the DOX-resistant and -sensitive hormone-refractory prostate cancer.

## Materials and methods

### Cell cultures

Human prostate cancer DU145 cell line was provided from the Cell Bank of Ferdowsi University of Mashhad and maintained in RPMI-1640 (Biosera, France). Furthermore, human foreskin fibroblasts (HFF) were a gift from Tissue Engineering Laboratory in the Department of Biology, Ferdowsi University of Mashhad, which were cultured in DMEM (Biosera, France). Both media were supplemented with 10% FBS, 100 U mL<sup>-1</sup> penicillin, and 100 µg mL<sup>-1</sup> streptomycin.

### Establishment of DOX-resistant DU145 cells

In order to establish the DU1454/DOX20 subline, DU145 cells were first cultured in the RPMI1640 medium containing 10 nM DOX (Venus Remedies Limited companies, Iran) for 6 days and the drug concentration was doubled. The DU145 cells could survive and grow exponentially in the medium containing 20 nM DOX for more than 1 month, whereas they could not grow in the presence of 40 nM DOX and gradually detached from the bottom of flasks after less than 6 days of culture [20]. The established cells that were survived in 20 nM concentration of DOX were named as DU1454/DOX20 cells. All experiments were performed

with DU1454/DOX20 cells continuously cultured in 20 nM DOX for 1–2 weeks.

### Cell viability assay

The influence of CIP (Samen Pharmaceutical, Iran) and DOX on the viability of DU145 and DU145/DOX20 cells was assessed using MTT (Sigma Aldrich, USA) assay. The 24-h-cultured DU145 cells were exposed with the various doses of CIP (12.5–100 µg mL<sup>-1</sup>) for different time periods. The cells were also treated with different concentrations of DOX (10–1500 nM) for 48 h in order to determine the IC<sub>50</sub> values of DOX against DU145 and DU145/DOX20 cells. HFF cells was considered as control normal cells. Additionally, DU145 and DU1454/DOX20 cells were treated with 5 and 25 µg mL<sup>-1</sup> CIP in the absence or existence of 20 nM DOX. The cells cultured in medium without CIP in the absence or presence of 20 nM DOX were considered as the controls. After each treatment, MTT solution (10 µL, 5 mg mL<sup>-1</sup>) was added to each well. The cultured supernatant was replaced with DMSO after 4 h. The absorbance at 570 nm was measured using an ELISA reader (BioTek, ELX800, USA) and the percentage of cell viability was calculated using Eq. 1. The values of half maximal inhibitory concentration (IC<sub>50</sub>) of each drug were determined based on the semi-logarithmic dose–response curves by GraphPad Prism 6 software [21].

%Cell viability

$$= \left( \frac{\text{OD}_{570} \text{ of treated cells} - \text{OD}_{570} \text{ of background}}{\text{OD}_{570} \text{ of control (untreated) cells} - \text{OD}_{570} \text{ of background}} \right) \times 100 \quad (1)$$

### Wound-healing assay

The wound-healing assay was performed to evaluate the influence of FBS on the migration potential of DU145 cells and the efficacy of CIP and DOX on the wound closure ability of DU145 and DU145/DOX20 cells. For this purpose, the cells (at a density of 1 × 10<sup>5</sup> cells per well) were cultured in 6-well plates. After 48 h incubation, an artificial homogeneous wound was introduced using a sterile yellow micropipette tip in the center of the monolayer cells and then the cells were cultured in medium with or without FBS. To explore the effect of drugs on the cell migration, the cells were treated with FBS-free medium containing CIP (5 and 25 µg mL<sup>-1</sup>) and DOX (20 nM), alone or in combination, immediately after scratching. The wound area of each treatment was photographed immediately after wound incision and then every day for 2–3 days on an inverted microscope (LABOMED iVu3000-TCM400, Germany) at ×40 magnification. The scratch area was measured by ImageJ 1.44

software and migration percentage was obtained using Eq. 2 [22].

$$\begin{aligned} &\text{Cell migration(\%)} \\ &= \left( \frac{\text{Wound area after wounding} - \text{Wound area at various times after wounding}}{\text{Wound area after wounding}} \right) \\ &\times 100 \end{aligned} \tag{2}$$

### Clonogenic survival assay

Clonogenic survival assay was performed to assess the effect of CIP (5 and 25 µg mL<sup>-1</sup>) and DOX (20 nM) on the clonogenicity of DU145 and DU145/DOX20 cells. In this regard, the cells (500 and 500–100,000 cells per well of a 24-well plate for DU145 and DU145/DOX20 cells, respectively) were treated with drugs alone or combination of both for 9 days, fixed with methanol, and stained with 0.5% crystal violet. Then, the number of colonies was counted and the plating efficiency percentage (P.E.%) was calculated using Eq. 3 [23].

$$\text{Plating efficiency(\%)} = \frac{\text{Number of colonies formed}}{\text{Number of cells seeded}} \times 100 \tag{3}$$

### Spheroid formation assay

The cells (1000 cells per well) were cultured on the 0.5% low-melting agarose-coated wells of a 96-well plate for 24 h. The cell aggregates were then collected, mixed with 0.24 mg mL<sup>-1</sup> collagen (Corning, Life Sciences, USA), and transferred to 0.5% agarose-coated wells. After a 30-min incubation, a culture medium containing CIP (5 and 25 µg mL<sup>-1</sup>) with or without DOX (20 nM) was added to each well and incubated at 37 °C. The cells cultured in medium without CIP in the absence or presence of 20 nM DOX were considered as controls. Spheroids were photographed immediately after seeding (day 0) and then every day for 8 days using an inverted microscope (LABOMED iVu3000-TCM400, Germany). The size and relative area of spheroids were, respectively, determined using ImageJ 1.44 software and Eq. 4 [24].

$$\text{Relative spheroid area} = \frac{\text{Spheroid area at various post-seeding times}}{\text{Spheroid area on day 3 after seeding}} \tag{4}$$

### Transporter activity assays

DOX is known to transport by ATP-binding cassette B1 transporter (ABCB1) [25]. The activity of ABCB1 transporter in DU145 and DU145/DOX20 cells was assessed through determining the intracellular accumulation of

Hoechst 33342, rhodamine 123 (Rho 123), and DOX, which are fluorescent substrates for ABCB1, as described earlier with some modifications [26–28]. For the Hoechst 33342 efflux assay, the 48 h-cultured cells were preincubated with transport assay buffer (5.3 mM KCl, 1.1 mM KH<sub>2</sub>PO<sub>4</sub>, 0.8 mM MgSO<sub>4</sub>, 1.8 mM CaCl<sub>2</sub>, 11 mM D-glucose, 10 mM HEPES, and 136 mM NaCl, pH 7.4). After 20 min of incubation at 37 °C, transport assay buffer was replaced with one containing 5 µg mL<sup>-1</sup> Hoechst 33342 (Invitrogen, USA) in the absence or presence of 50 µM verapamil (an inhibitor of ABCB1). Assay was stopped by the addition of ice-cold transport assay buffer at 90 min of incubation at 37 °C [29, 30]. The cellular accumulation of Hoechst 33342 was measured at an excitation wavelength of 360 nm and an emission wavelength of 460 nm using Synergy Multi-Mode Reader (BioTek) and expressed as mean of arbitrary units (a.u.). For Rho 123 and DOX accumulation assays, a total of 3 × 10<sup>5</sup> cells were incubated with 10 µg mL<sup>-1</sup> Rho 123 (Sigma, Germany) or 20 nM DOX for 60 min and 120 min, respectively, in the dark at 37 °C and 5% CO<sub>2</sub>. After twice washing with PBS, the cells were resuspended in 0.5 mL of PBS and the fluorescence intensity of the intracellular Rho 123 and DOX was detected by a BD FACSCalibur flow cytometer (Becton Dickinson Biosciences, San Jose, CA) at 530 nm (FL1) and 580 nm (FL2), respectively, and data were analyzed using FlowJo software (version 7.6.1).

### Quantification of ATP-binding cassette sub-family C member 4 (ABCC4) through using qRT-PCR

The mRNA expression of efflux transporter ABCC4 was quantified through applying comparative relative real-time PCR. Briefly, 1 µg of total purified RNA was transcribed into cDNA with random primers using a first-strand synthesis cDNA kit (Parstous, Iran). Quantitative real-time PCR was performed in duplicate reactions using SYBR Green detection (AMPLIQON, Denmark) on a LightCycler® 96 Real-Time PCR System thermocycler (Roche, Germany). The expression was normalized using glyceraldehyde-3-phosphate dehydrogenase (GAPDH). Primers utilized in PCR include ABCC4 forward: 5'-GAAATTGGACTTCAC GATTTAAGG-3', reverse: 5'-TTCCACAGTTCCTCATCC GT-3'; GAPDH forward: 5'-GGAAGGTGAAGGTCGGAG TCA-3', reverse: 5'-GTCATTGATGGCAACAATATCCAC T-3'. Furthermore, the PCR was run at 95 °C for 15 min, followed by 40 cycles of 95 °C for 15 s, 59 °C for 20 s, and 72 °C for 20 s. The relative quantification of ABCC4 expression was analyzed through using the 2<sup>-ΔΔCt</sup> method. In the present study, the mRNA expression higher or less than one-fold relative to the corresponding gene expression in DU145 cells was considered as overexpression or underexpression, respectively [31].

## Statistical analysis

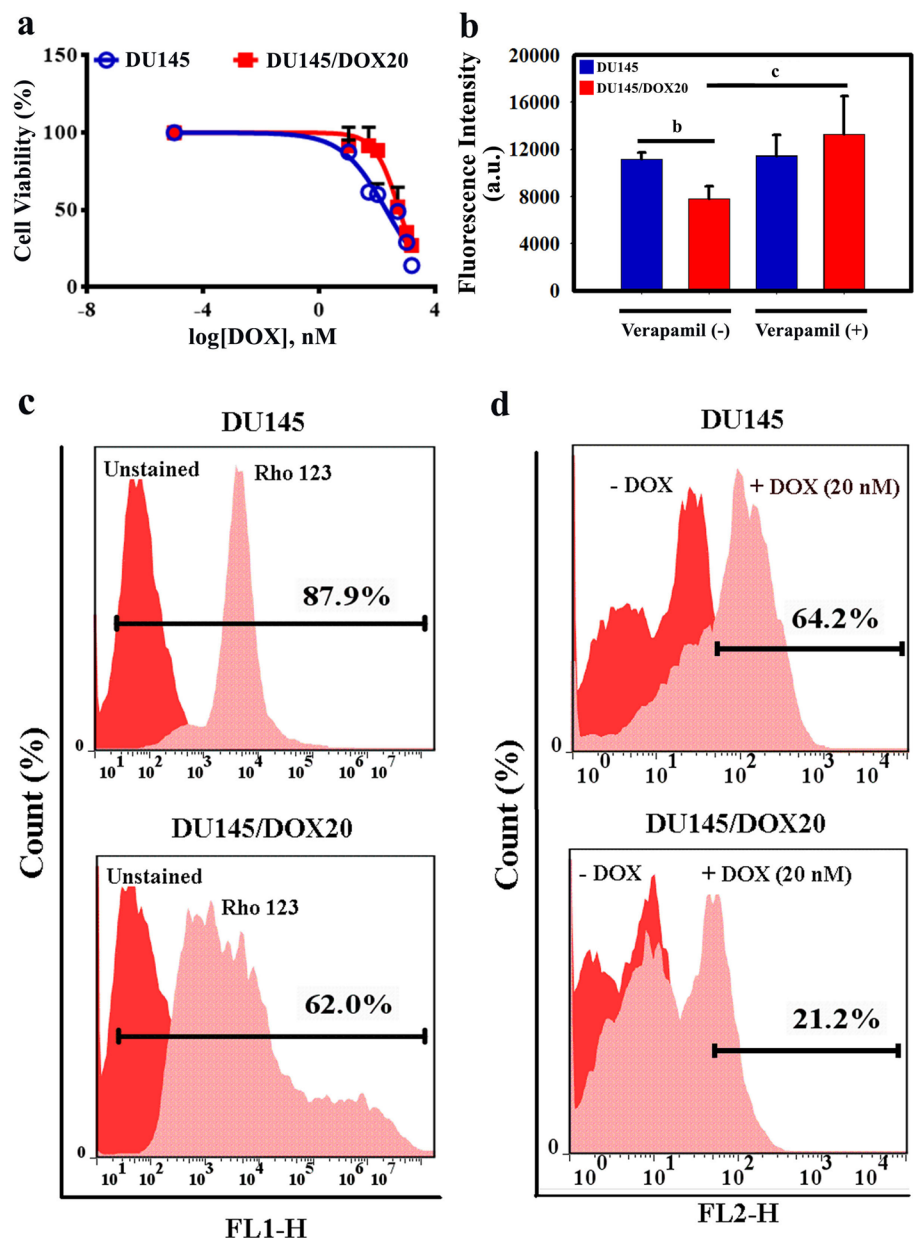
The statistical significance was determined through employing One-way ANOVA and the Student's *t*-test using Graph-Pad Prism 6 software and  $p < 0.05$  was considered as significant. All data from a minimum of three independent experiments with at least three wells for each condition were expressed as mean  $\pm$  SEM (or SD).

## Results

### Establishment of DOX-resistant DU145 Cells

DOX-resistant DU145/DOX20 cells were established by exposing the parental DU145 cells to twofold increasing concentrations of DOX. DU145 cells were able to grow exponentially in the presence of 20 nM DOX even after 1 month, although the adhesion ability of DU145/DOX20 cells decreased compared to the parental DU145 cells. We found that the parental cells could not survive in the medium containing 40 nM DOX after 6 days and gradually detached from the bottom of flasks. As shown in Fig. 1a, the IC<sub>50</sub>

**Fig. 1** The IC<sub>50</sub> graphs of DU145 and DU145/DOX20 cells treated with various concentrations of doxorubicin (DOX) (a). Average Hoechst 33342 fluorescence intensity (arbitrary units, a.u.) for DU145 and DU145/DOX20 cells in the absence or presence of verapamil (b). Data show the means  $\pm$  SD of three independent experiment. b:  $p < 0.01$  and c:  $p < 0.001$ . Accumulations of rhodamine (Rho 123) (c) and doxorubicin (DOX) (d) in DU145 and DU145/DOX20 cells as determined using flow cytometry and one of representative flow cytometry histogram from three independent experiments is presented



value of DOX in DU145/DOX20 cells ( $569.5 \pm 53.8$  nM) was about twofold higher than that in DU145 ones ( $284.5 \pm 83.7$  nM) ( $p=0.04$ ), indicating a lower susceptibility of DU145/DOX20 cells to the cytotoxic activity of DOX. Given the overexpression of some ATP-binding cassette (ABC) membrane transporters in cancer chemotherapy resistance and the role of ABCB1 in DOX resistance, hence, we examined the ABCB1 activity in both DU145 and DU145/DOX20 cells with the fluorescent P-glycoprotein (Pgp) substrates, Hoechst 33342, Rho 123, and DOX [32–34]. As evident in Fig. 1b, the fluorescence intensity of Hoechst 33342 in DU145/DOX20 cells was lower than that in DU145 cells ( $p < 0.01$ ). Moreover, the fluorescence intensity was markedly increased in DU145/DOX20 cells (68%) by verapamil treatment ( $p < 0.001$ ), whereas its fluorescence level in DU145 cells was enhanced to a lesser extent ( $p > 0.05$ ). The results of Rho 123 and DOX accumulation assay showed that they were markedly accumulated in the parental DU145 cells, more than those observed in

DU145/DOX20 cells (Fig. 1c, d). These data indicate that the ABCB1 transporter was functionally more active in this DOX-resistant sub-line of DU145 cells than in the parental DU145 cells. We also found that some of DU145/DOX20 cells exhibited morphological changes such as becoming flatter and larger than DU145 cells and some appeared multinucleated (Fig. 2a). In addition, we assessed intracellular granularity by flow cytometry. Through this analysis, we observed an increase in the granularity of DU145/DOX20 cells ( $21.70 \pm 5.23\%$ ) compared to the parental DU145 cells ( $5.84 \pm 0.23\%$ ) ( $p < 0.05$ ) (Fig. 2b).

**Cytotoxicity assay**

The MTT results represented that CIP reduced the proliferation of DU145 cells in a time- and concentration-dependent manner. As evident in Table 1, the IC<sub>50</sub> values of CIP for DU145 cells were much higher than those for DU145/DOX20 cells. Additionally, IC<sub>50</sub> values against DU145 and

**Fig. 2** Representative phase contrast images of the parental DU145 cells and DU145/DOX20 cells (×40 magnification). Red circles indicate enlarged binucleated and multinucleated cells containing five nuclei, respectively (a). Dot plots of size distribution (SSC side scatter) versus granularity (FSC forward scatter) of DU145 and DU145/DOX20 cells generated from flow cytometric analysis of levels of granularity (b)

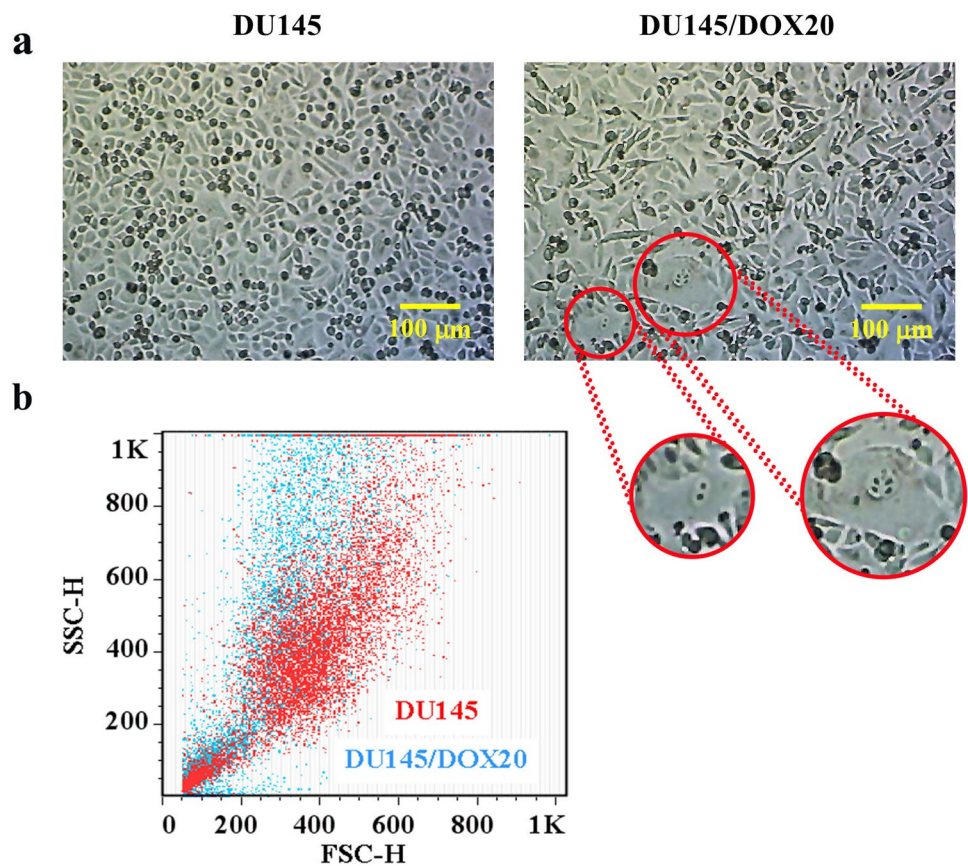


**Table 1** IC<sub>50</sub> values (μg mL<sup>-1</sup>) for DU145 and DU145/DOX20 cells treated with ciprofloxacin at various time points

Time (days)	1	2	3	5	7	9
DU145	177.3 ± 5.9	105 ± 4.3	48.2 ± 0.4	36.57 ± 5.5	47.07 ± 8	37.1 ± 6.7
DU145/DOX20	65.1 ± 15.8	35.3 ± 3.6	44.8 ± 5.8	19.9 ± 5.9	23.6 ± 4.7	15.6 ± 0.13

DU145/DOX20 cells decreased during the first 3 and 5 days, respectively, and then remained constant. DU145/DOX20 cells exhibited lower  $IC_{50}$  values compared to the parental DU145 cells. The  $IC_{50}$  concentration of CIP on normal HFF cells at 48 h ( $443.5 \pm 63.4 \mu\text{g mL}^{-1}$ ) was significantly higher than that on DU145 ones ( $105.0 \pm 4.3 \mu\text{g mL}^{-1}$ ) ( $p=0.02$ ), indicating that CIP is safe without obvious cytotoxicity to normal cells. Two concentrations of CIP,  $5 \mu\text{g mL}^{-1}$  (serum concentration) [35] and  $25 \mu\text{g mL}^{-1}$  ( $1/4 IC_{50}$ ) for which cell viability remained higher than 75% after 48 h of exposure, were selected for next experiments. The viability of DU145 and DU145/DOX20 cells treated with CIP (5 and  $25 \mu\text{g mL}^{-1}$ ) in the absence or presence of DOX (20 nM) is shown in Fig. 3a and b, respectively. We found that CIP ( $5 \mu\text{g mL}^{-1}$ ) alone and DOX alone had no obvious effect on the viability of DU145 cells over the first 2 days, whereas their combination significantly reduced the cell viability during this period (Fig. 3a). Further, a significant reduction was observed in the viability of DU145 cells treated with CIP (5 and  $25 \mu\text{g mL}^{-1}$ ) and DOX, alone or in combination, from Day 3 to Day 5. As displayed in Fig. 3b, the inhibitory effect of CIP on the proliferative potential of DU145/DOX20 cells was also time- and concentration-dependent in both the absence and presence of 20 nM DOX. CIP alone (5 and  $25 \mu\text{g mL}^{-1}$ ), but not DOX alone, had inhibitory effect on the viability of DU145/DOX20 cells over the experimental time period of 5 days. Moreover, no significant difference was observed between the viability of the CIP-exposed DU145/DOX20 cells in the absence or presence of 20 nM DOX during the first 2 days, indicating the effectiveness of CIP alone in reducing the viability of DU145/DOX20 cells

within 48 h. The combination of 25 or  $5 \mu\text{g mL}^{-1}$  CIP with 20 nM DOX resulted in a higher reduction in the viability of DU145/DOX20 cells as compared to either treatment alone since the 3rd and 4th day of treatment, respectively. These findings reflected that CIP could improve the sensitivity of the DU145/DOX20 cells to DOX after 2–3 days of exposure. Furthermore, both concentrations of CIP (5 and  $25 \mu\text{g mL}^{-1}$ ) led to a significantly higher reduction in the viability of DU145/DOX20 cells compared to the parental DU145 cells, indicating higher sensitivity of DU145/DOX20 cells to CIP.

### Wound-healing assay

Figure 4 depicts the results of wound-healing assay on the DU145 cells treated with CIP (5 and  $25 \mu\text{g mL}^{-1}$ ) alone or in combination with DOX (20 nM). Given that previous studies have shown that FBS can induce cell migration [36]. The motility of DU145 cells was first assessed in both the existence and absence of FBS. The scratch closure of DU145 cells occurred at a faster rate in the presence of FBS compared with its absence (complete wound closure after 2 days versus 3 days of incubation) (Fig. 4a), indicating that cell migration significantly increased in the presence of FBS. The stimulatory effect of serum on the cell migration is probably due to the proliferative activity of FBS [37, 38]. Further, we performed all wound-healing assays in FBS-free medium for 2 days because DOX (20 nM) alone exhibited no significant toxicity on both cell types during the first 48 h of treatment. CIP alone and DOX alone had a clear negative effect on

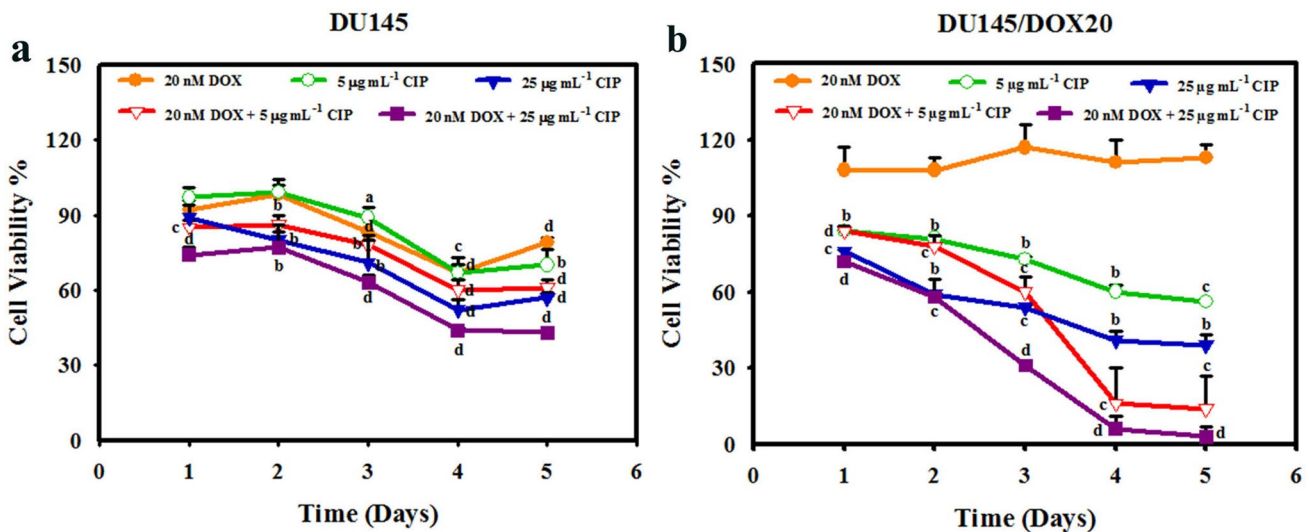
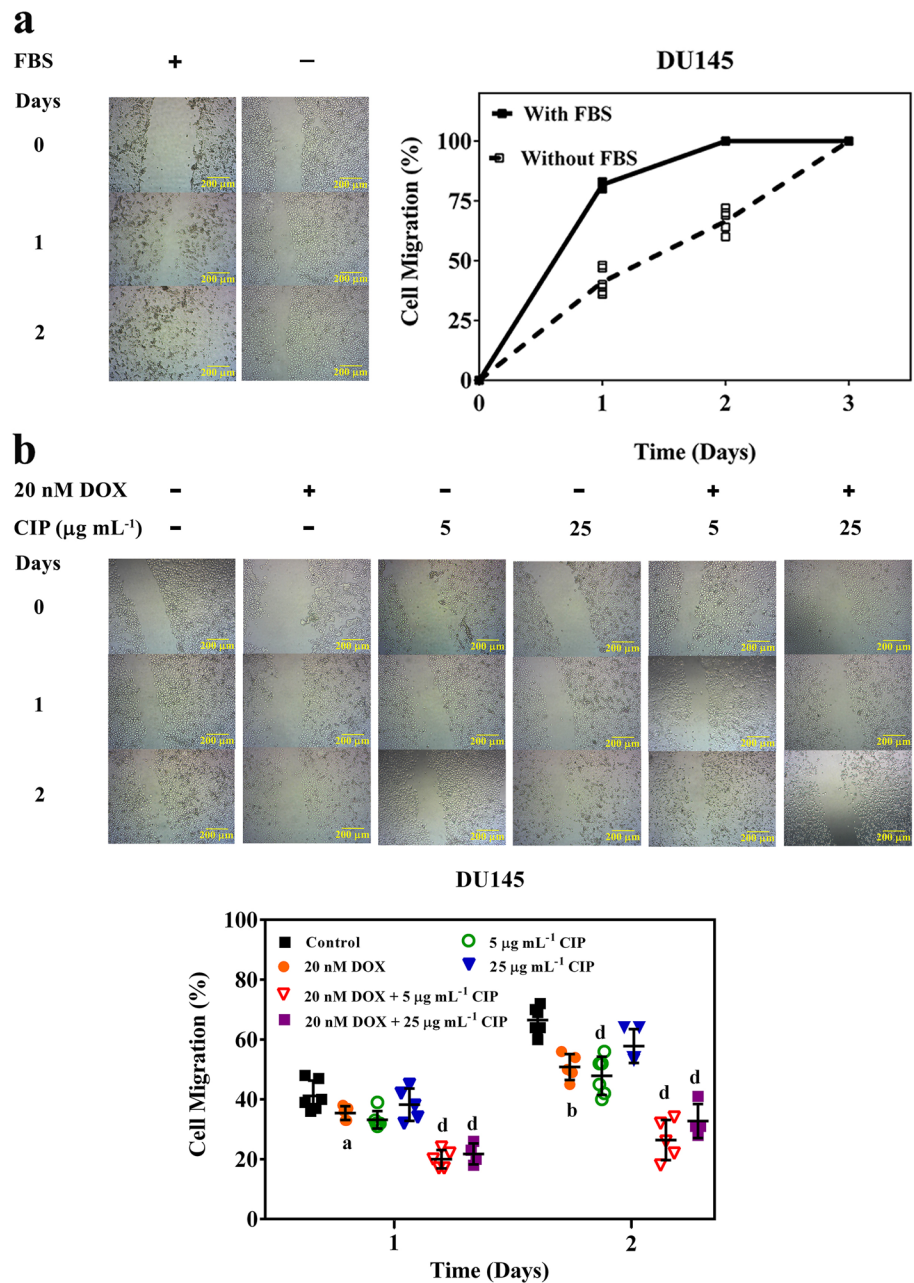


**Fig. 3** Time course changes in the viability of DU145 cells treated with CIP (5 and  $25 \mu\text{g mL}^{-1}$ ) in the absence or presence of 20 nM DOX (a). The viability of DU145/DOX20 cells treated with 5 and

$25 \mu\text{g mL}^{-1}$  CIP in the absence or presence of 20 nM DOX (b). a:  $p < 0.05$ , b:  $p < 0.01$ , c:  $p < 0.001$ , and d  $p < 0.0001$  vs. untreated cells. Data show the means  $\pm$  SEM of three independent experiment

**Fig. 4** The influence of FBS and ciprofloxacin (CIP) on the migration ability of DU145 cells. Representative images of in vitro wound-healing assay taken at 0–3 days post-wounding ( $\times 40$  magnification) and the percentage of migration for DU145 cells in the presence or absence of FBS (a). Representative images of in vitro wound-healing assay taken at 0–2 days post-wounding ( $\times 40$  magnification) and the percentage of migration for CIP-treated DU145 cells in the absence of FBS without or with 20 nM doxorubicin (DOX) (b). a:  $p < 0.05$ , b:  $p < 0.01$ , and d:  $p < 0.0001$  vs. control (untreated) cells. Data show the means  $\pm$  SD of three independent experiments



the migration of the parental cells at 2-day post-wounding ( $p < 0.0001$  for  $5 \mu\text{g mL}^{-1}$  CIP and  $p < 0.01$  for 20 nM DOX) (Fig. 4b). The combination of CIP with DOX led to a more severe decrease in the wound closure rate of DU145 cells ( $p < 0.0001$ ). No significant effect on the wound closure ability of DU145/DOX20 cells by CIP and DOX alone was observed at 2-day post-wounding (Fig. 5), whereas exposure of DU145/DOX20 cells to a combination of  $25 \mu\text{g mL}^{-1}$  of CIP and DOX resulted in a significant decrease in the extent of cell migration.

### Clonogenic survival assay

Figure 6 represents the results related to the clonogenic assay of DU145 cells. DOX (20 nM) inhibited the colony formation ability of DU145 cells by 89%, while CIP ( $5$  and  $25 \mu\text{g mL}^{-1}$ ) treatment resulted in an increase in their clonogenic potential. Additionally, the exposure of DU145 cells with CIP in combination with DOX prevented colony formation. The efficacy of CIP on the colony formation ability of DU145/DOX20 cells in the absence or presence of 20 nM

**Fig. 5** The impact of ciprofloxacin (CIP) on the migration ability of DU145/DOX20 cells. Representative images of in vitro wound-healing assay taken at 0–2 days post-wounding (×40 magnification) and the percentage of cell migration for DU145/DOX20 cells in the absence of FBS without or with 20 nM doxorubicin (DOX). a:  $p < 0.05$  and b:  $p < 0.01$  vs. control (untreated) cells. Data show the means ± SD of three independent experiments

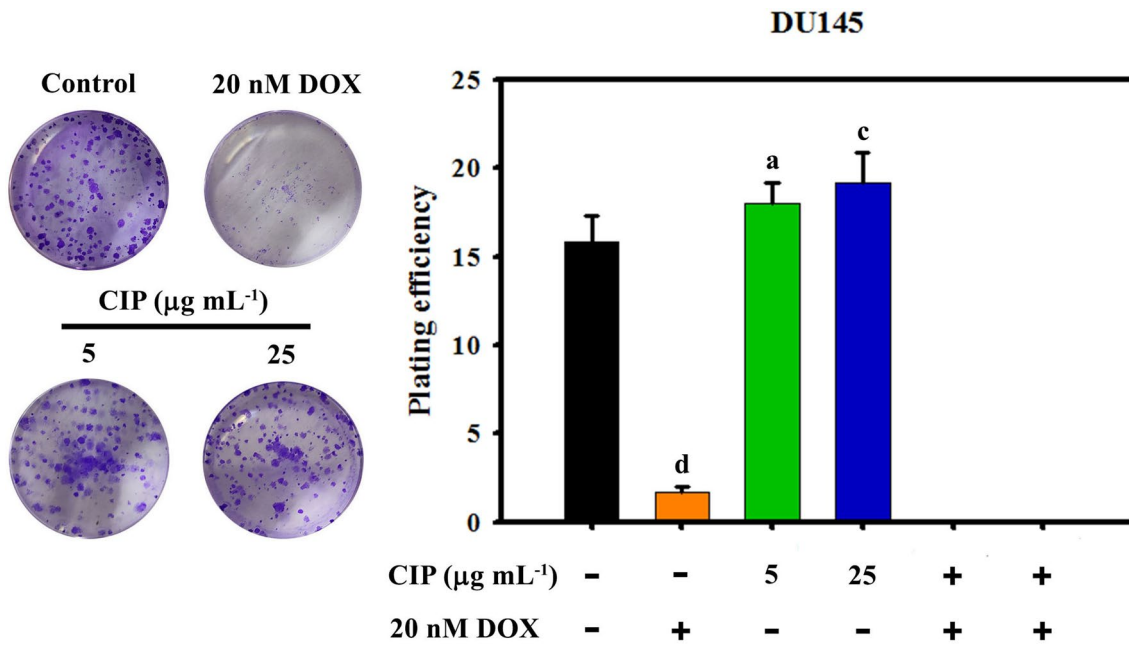
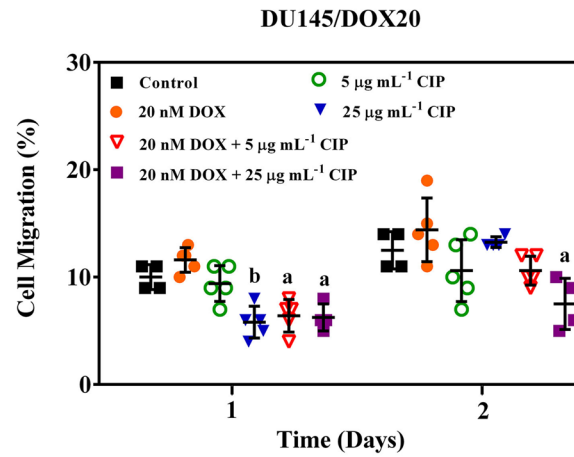
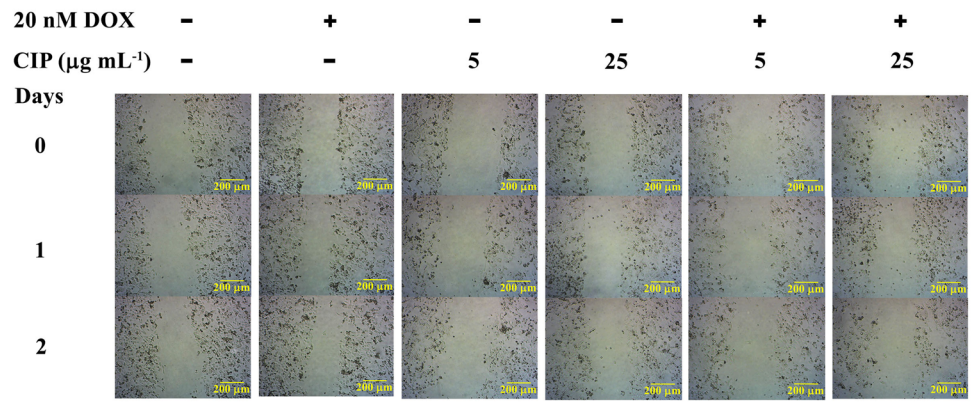


**Fig. 6** Representative images of colony formation assay and the plating efficiency (%) of DU145 cells treated with ciprofloxacin (CIP) in the absence or presence of 20 nM DOX. a:  $p < 0.05$ , c:  $p < 0.001$ , and

d:  $p < 0.0001$  vs. control (untreated) cells. Data show the means ± SD of three independent experiments

DOX was performed with the cell seeding density ranging from 500 to 100,000 cells per well. At lower cell densities ( $< 1 \times 10^5$  cells per well), the cells were detached from the plate surface a few days after plating and no colony was detected over 9 days. The colonies were adjacent to each other and no single colony was observed at high cell density ( $1 \times 10^5$  cells per well) even in 2 days.

### Spheroid culture

The results of spheroid formation assay are illustrated in Fig. 7. As shown, the relative area of DU145 and DU145/DOX20 spheroids enhances over 8 days, which is statistically significant only for DU145 spheroids ( $p < 0.0001$ , day 2 versus days 6 and 8;  $p < 0.001$ , day 4 versus day 6;  $p < 0.0001$ , day 4 versus day 8;  $p < 0.0001$ , day 6 versus day 8). In addition, the relative area of DU145 spheroids

(from  $1.82 \pm 0.29$  to  $12.47 \pm 2.61$ ) was increased more than that of DU145/DOX20 cells (from  $1.28 \pm 0.23$  to  $1.94 \pm 0.51$ ). Treatment with DOX (20 nM) and CIP ( $5$  and  $25 \mu\text{g mL}^{-1}$ ) alone could significantly decrease the growth of DU145 spheroids at 8 day after seeding ( $p < 0.0001$ ) (Fig. 7a). There was no significant difference between the area of the DU145 spheroids treated with  $5 \mu\text{g mL}^{-1}$  CIP alone and those exposed to its combination with DOX, while the combination of  $25 \mu\text{g mL}^{-1}$  CIP and DOX prevented the spheroid formation. Further, no difference was observed between the area of the DU145/DOX20 spheroids exposed or not exposed to 20 nM DOX (Fig. 7b). The size of the DU145/DOX20 spheroids does not decline in the existence of CIP or DOX. Furthermore, DOX and CIP ( $5$  and  $25 \mu\text{g mL}^{-1}$ ) combination treatment resulted in no spheroid formation at all, indicating that their combination effectively suppressed the growth of spheroids in 3D cultures.

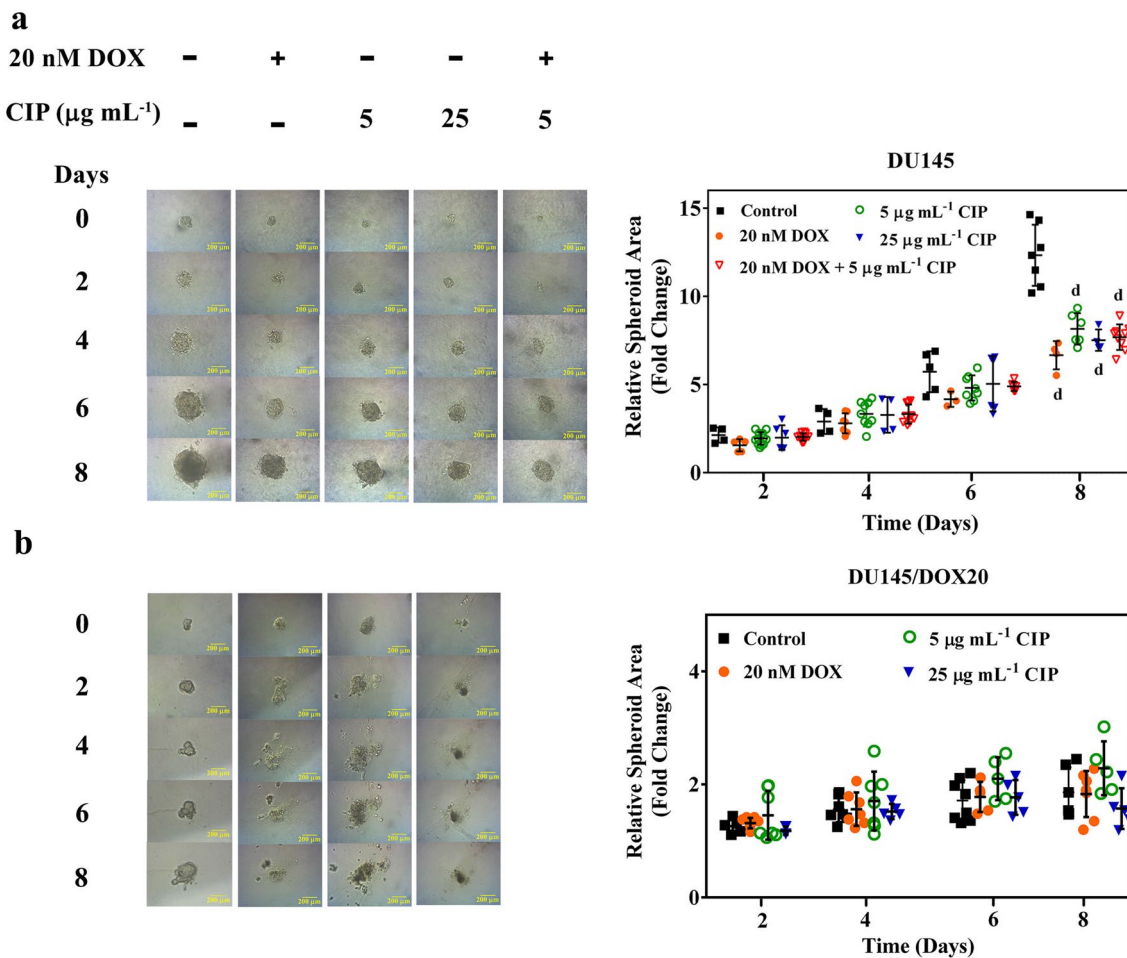


**Fig. 7** The influence of ciprofloxacin (CIP) on the growth of DU145 and DU145/DOX20 spheroids over 8 days. Representative images ( $\times 100$  magnification) and the relative area of DU145 (a) and DU145/

DOX20 (b) spheroids treated with CIP in the absence or presence of 20 nM doxorubicin (DOX). d:  $p < 0.0001$  vs. control (untreated) cells. Data show the means  $\pm$  SD of three independent experiments

## ABCC4 expression

We analyzed the mRNA expression of *ABCC4* in DU145 and DU145/DOX20 cells in order to study the CIP efflux transporter. No substantial difference in the *ABCC4* mRNA expression level between both cell types was observed (Supplementary Fig. 1).

## Discussion

DOX, one of the most effective chemotherapeutic drugs against a variety of cancers, can induce drug resistance through various mechanisms, such as drug efflux pump ABCB1 [39]. Active DOX efflux in drug-resistant cells results in reduced its intracellular accumulation and antitumor efficacy. CIP, as a potential antibiotic for genitourinary cancer treatment, has been reported to sensitize HRPC cell lines (PC-3 and LNCaP) to DOX at millimolar concentrations [18]. In the present study, the effect of micromolar concentrations of CIP [ $5 \mu\text{g mL}^{-1}$  ( $15.1 \mu\text{M}$ ) and  $25 \mu\text{g mL}^{-1}$  ( $75.4 \mu\text{M}$ )] was assessed on the cell proliferation, migration potential, colony formation capacity, and spheroid growth of the acquired DOX-resistant DU145 cells. We showed that the DU145/DOX20 cells was considerably more sensitive to CIP than the parental DU145 cells. The combination of CIP with DOX resulted in a significant decrease in the viability and no spheroid formation of DU145/DOX20 cells.

DU145 cells, as a model of androgen-independent prostate cancer cells, were continuously exposed with the increasing concentrations of DOX to establish the acquired DOX-resistant DU145 sub-cell line (DU145/DOX20). DU145/DOX20 cells had a twofold higher  $\text{IC}_{50}$  value for DOX than the parental DU145 cells, indicating a decreased sensitivity of DU145/DOX20 cells to DOX. This finding was confirmed by efflux transporter activity assays, which showed higher ABCB1 transporter activity for DOX in DU145/DOX20 cells relative to DU145 cells. Further, the adhesive capacity of DU145/DOX20 cells decreased compared to that of DU145 ones so that DU145/DOX20 cells at low densities were detached from the plate surface a few days after plating. This transformation may be related to the epithelial–mesenchymal transition (EMT) process which is characterized by cell morphology change from epithelial round phenotype to mesenchymal spindle-shaped phenotype and reduction in cell–cell adhesion [40]. In addition, DU145/DOX20 cells represented morphological changes such as enlarged and flattened shape, which is in line with the results of Shankaranarayanan et al. [41]. Furthermore, a considerable of DU145/DOX20 cells were multinucleated, known as polyploid giant cancer cells (PGCCs) or poly-aneuploid cancer cells (PACCs), which may be attributed to the increased stress. A similar finding was reported by Amend et al., who

observed the formation of PGCCs after 72 h exposure of PC-3 cells with LD90 docetaxel [42]. PGCCs have been documented as emerging in response to stress, like the replicative stress occurring after exposing to chemotherapeutic drugs. These cells are associated with metastasis and exhibit resistance to anticancer therapy, and therapeutically targeting them is of utmost importance [43–46].

The MTT results indicated that CIP resulted in decreasing the growth of DU145 and DU145/DOX20 cells in a time- and dose-dependent manner. In addition, the  $\text{IC}_{50}$  value of CIP against the normal HFF cells was significantly higher than that of DU145 ones, which suggests that CIP can be considered as an adjuvant for prostate cancer therapy without side effects on normal cells. This result is in agreement with that obtained by Aranha et al., which demonstrated the significant less efficacy of CIP on the growth of normal prostate epithelial cells (MLC8891) compared to the PC3 ones [13]. In the present study, the antiproliferative activity of CIP on the DOX-resistant DU145 cells was reported for the first time. The growth inhibitory effect of CIP on DU145/DOX20 cells was more than that on DU145 ones in both the absence and presence of 20 nM DOX, which reflects the greater susceptibility of DU145/DOX20 cells to CIP in 2D culture. DOX at 20 nM concentration had no cytotoxicity against DU145/DOX20 cells over the experimental time period and no significant difference was observed between the viability of CIP-treated DU145/DOX20 cells in the absence or in the presence of 20 nM DOX during the first 2 days. However, the combination of DOX with  $25 \mu\text{g mL}^{-1}$ , or with  $5 \mu\text{g mL}^{-1}$  CIP resulted in greater efficacy than either drug alone since the 3rd and 4th day of treatment, respectively. Our findings are consistent with previous studies that indicated the chemosensitizing effect of CIP to ABCB1 substrates [17, 18]. Based on the results of the previous studies, chemoresistant cells require more ATP to maintain drug efflux transporters activity, as well as the homeostasis of survival pathways under stress conditions [47]. An increased intracellular ATP in chemoresistant cell lines may be caused by enhancing aerobic glycolysis and mitochondrial ATP synthesis [48]. CIP impairs mitochondrial DNA replication and transcription, and leads to mitochondrial respiratory chain dysfunction, which in turn reduces the intracellular ATP level [10]. Indeed, Koziel et al. [49] reported that  $25 \mu\text{g mL}^{-1}$  CIP resulted in decreasing ATP content and capacitive  $\text{Ca}^{2+}$  entry in Jurkat cells.

ABCC4 (Mrp4), a CIP transporter, is widely expressed in neoplastic prostate epithelial cells and gradually down-regulated during malignant tumor progression [50]. We proposed that the greater sensitivity of DU145/DOX20 cells to CIP compared to the parental cells may be related to a decrease in *ABCC4* expression. For this purpose, the mRNA abundance of *ABCC4* in the parental DU145 and DU145/DOX20 cells was determined using qRT-PCR. We observed

a slight, non-significant decrease in the mRNA expression of *ABCC4* in DU145/DOX20 cells compared to DU145 cells (Fold change = -0.08). It seems that the mRNA expression level of *ABCC4* transporter offers no explanation of susceptibility of DU145/DOX20 cells to CIP. Given that CIP has been known to have a protein binding efficiency of 20–30% [51] and probably able to diffuse in the various subcellular compartments such as lysosome [52]; therefore, the sensitizing effect of CIP can be likely related to the increased retention time of CIP in cells through intracellular distribution and compartmentalization or binding to still-undefined cellular constituents such as soluble proteins [53]. Moreover, several reports revealed that CIP stimulated the ATPase activity of ABCB1 by competitively binding to the ATP-binding site and inhibiting drug efflux function [17]. The present findings also indicate that the DOX resistance of DU145/DOX20 cells may be *ABCC4* expression-independent. These results are in line with those of the previous ones which demonstrated the irresponsibility of *ABCC4* for DOX resistance [54].

Additionally, the plating efficiency of DU145 cells was determined  $16.0 \pm 1.0\%$ , which is consistent with the results of the previous studies [55]. The results of colony formation assay indicated the decrease of the colony forming ability of DU145 cells exposed to DOX (20 nM). Further, CIP (5 and  $25 \mu\text{g mL}^{-1}$ ) caused an increase in the clonogenicity of DU145 cells. Phiboonchaiyanan et al. reported an increase in the colony number of human non-small cell lung cancer (NSCLC) cells pretreated with CIP at non-toxic concentrations ( $2.5$  and  $5 \mu\text{g mL}^{-1}$ ) [35], which confirms the results of the present study. They suggested that CIP induces cancer stem cells phenotypes in NSCLC cells. The plating efficiency of DU145/DOX20 cells could not be estimated due to their low adhesive potential.

Further, we found that scratch wounds in DU145 and DU145/DOX20 cells were closed by  $67.0 \pm 5.0\%$  and  $13.0 \pm 2.0\%$  at 48 h, respectively. The observed low migration ability of DU145/DOX20 cells may be due to their low adhesion properties. Exposure with CIP alone and DOX alone led to a marked reduction in the motility of the parental DU145 cells at 2-day post-wounding time point, and a more severe decrease in the migration was observed in combination treatment. DOX alone had no significant effect on the wound closure ability of DU145/DOX20 cells over a period of 2 days, while its combination with  $25 \mu\text{g mL}^{-1}$  CIP resulted in an obvious decrease in their scratch closure rate within 2 days post-wounding. These data indicated the inhibitory effect of CIP on the cell migration induced by DOX. Previous studies have shown a direct relationship between mitochondrial membrane potential and drug resistance and suggested mitochondrial activity inhibition is considered as a promising strategy to prevent metastasis in the drug-resistant cancer cells [56].

Analysis of spheroid images showed an increase in the average diameter of the parental DU145 spheroids from  $170 \pm 29 \mu\text{m}$  on day 0 to  $523 \pm 55 \mu\text{m}$  on day 8. As large spheroids (with diameter over  $500\text{--}600 \mu\text{m}$ ) tend to form the necrotic core due to limited nutrient diffusion and severe hypoxia, as well as the accumulation of waste products and decreased pH [57], the spheroid growth assay was conducted for a period of 8 days. Furthermore, we observed that CIP alone and DOX alone suppressed the growth of the parental DU145 spheroids, but not of DU145/DOX20 cells. There was no significant increase in the growth of DU145/DOX20 spheroids over 8 days. No spheroids were formed by DU145/DOX20 cells treated with the combination of 20 nM DOX and 5 or  $25 \mu\text{g mL}^{-1}$  of CIP and by DU145 cells exposed to DOX in the presence of  $25 \mu\text{g mL}^{-1}$  CIP. These results suggested that the combination of CIP with DOX may potentiate toxicity in both cell types. Finally, DU145 and DU145/DOX20 cells were more resisted to CIP in 3D culture than 2D one, which may be related to the difference between 2 and 3D microenvironments, which profoundly influences drug diffusion. These results are in agreement with those of some studies which reflected that malignant cancer cells usually are more chemoresistant in 3D culture.

CIP is relatively non-toxic and presents a high volume of distribution. The recommended dose of CIP for chronic bacterial prostatitis is 500 mg orally or 400 mg intravenously every 12 h for 28 days. The maximum serum concentration of CIP after both administrations is  $3\text{--}5 \mu\text{g mL}^{-1}$  [51, 58]. CIP can be administered in high doses for longer periods of time (750 and 1000 mg for more than 1 week). Its serum concentration increases proportionately with doses up to 1000 mg and is not beyond  $7 \mu\text{g mL}^{-1}$  [59, 60]. Generally, CIP is widely distributed throughout the body, and prostate concentrations often exceed serum concentrations (2–2.45 times the plasma levels) [61]. The highest concentration of CIP, which can be achieved in the prostate, has been reported to be  $15 \mu\text{g mL}^{-1}$  [15]. CIP concentrations tested in this study were  $5 \mu\text{g mL}^{-1}$  and  $25 \mu\text{g mL}^{-1}$ , which were equal to its concentration in human plasma and 1.7 times higher than clinically achievable in prostatic tissue, respectively. Nevertheless,  $25 \mu\text{g mL}^{-1}$  concentration of CIP in the prostate might be achieved through targeted drug delivery systems to prostatic tumor cells [62].

In summary, we indicate the effect of CIP on resensitizing DOX-resistant DU145 cells to DOX treatment. The results of this study suggested the possible usefulness of CIP in treating the prostate cancer resistant and sensitive to DOX. Finally, additional studies are required to identify the mechanism(s) involved in the CIP-induced cytotoxic effects on DOX-resistant HRPC cells.

**Supplementary Information** The online version contains supplementary material available at <https://doi.org/10.1007/s12032-022-01787-9>.

**Acknowledgements** We thank Dr. MR Abbaszadegan and N Taghechian for their kind help with qRT-PCR assay.

**Author contributions** RJ: Designed and conducted the experiments, analyzed the data, and wrote the manuscript. ADA and JG: Performed cell biological experiments and analyzed the data.

**Funding** This work was supported by Ferdowsi University of Mashhad, grant number 3/44066. Razieh Jalal has received research support from Ferdowsi University of Mashhad.

## Declarations

**Competing interests** The authors have no relevant financial or non-financial interests to disclose.

## References

- Chen J, Chen B, Zou Z, Li W, Zhang Y, Xie J, et al. Costunolide enhances doxorubicin-induced apoptosis in prostate cancer cells via activated mitogen-activated protein kinases and generation of reactive oxygen species. *Oncotarget*. 2017. <https://doi.org/10.18632/oncotarget.22592>.
- Li S, Yuan S, Zhao Q, Wang B, Wang X, Li K. Quercetin enhances chemotherapeutic effect of doxorubicin against human breast cancer cells while reducing toxic side effects of it. *Biomed Pharmacother*. 2018. <https://doi.org/10.1016/j.biopha.2018.02.055>.
- Bai T, Liu Y, Li B. LncRNA LOXL1-AS1/miR-let-7a-5p/EGFR-related pathway regulates the doxorubicin resistance of prostate cancer DU-145 cells. *IUBMB Life*. 2019. <https://doi.org/10.1002/iub.2075>.
- Tacar O, Sriamornsak P, Dass CR. Doxorubicin: an update on anticancer molecular action, toxicity and novel drug delivery systems. *J Pharm Pharmacol*. 2013. <https://doi.org/10.1111/j.2042-7158.2012.01567.x>.
- Zahreddine H, Borden K. Mechanisms and insights into drug resistance in cancer. *Front Pharmacol*. 2013. <https://doi.org/10.3389/fphar.2013.00028>.
- Kim S-Y. Cancer energy metabolism: shutting power off cancer factory. *Biomol Ther*. 2018. <https://doi.org/10.4062/biomolther.2017.184>.
- Shahruzaman SH, Fakurazi S, Maniam S. Targeting energy metabolism to eliminate cancer cells. *Cancer Manag Res*. 2018. <https://doi.org/10.2147/CMAR.S167424>.
- Willcocks S, Huse KK, Stabler R, Oyston PC, Scott A, Atkins HS, et al. Genome-wide assessment of antimicrobial tolerance in *Yersinia pseudotuberculosis* under ciprofloxacin stress. *Microb Genomics*. 2019. <https://doi.org/10.1099/mgen.0.000304>.
- Boerema J-BJ, Dalhoff A, Debruyne FM. Ciprofloxacin distribution in prostatic tissue and fluid following oral administration. *Chemotherapy*. 1985. <https://doi.org/10.1159/000238308>.
- Hangas A, Aasumets K, Kekäläinen NJ, Paloheinä M, Pohjoismäki JL, Gerhold JM, et al. Ciprofloxacin impairs mitochondrial DNA replication initiation through inhibition of Topoisomerase 2. *Nucleic Acids Res*. 2018. <https://doi.org/10.1093/nar/gky793>.
- Gürbay A, Hincal F. Ciprofloxacin-induced glutathione redox status alterations in rat tissues. *Drug Chem Toxicol*. 2004. <https://doi.org/10.1081/dct-120037504>.
- Bush NG, Diez-Santos I, Abbott LR, Maxwell A. Quinolones: mechanism, lethality and their contributions to antibiotic resistance. *Molecules*. 2020. <https://doi.org/10.3390/molecules25235662>.
- Aranha O, Grignon R, Fernandes N, McDONNELL TJ, Wood DP, Sarkar FH. Suppression of human prostate cancer cell growth by ciprofloxacin is associated with cell cycle arrest and apoptosis. *Int J Oncol*. 2003. <https://doi.org/10.3892/ijo.22.4.787>.
- Yadav V, Talwar P. Repositioning of fluoroquinolones from antibiotic to anti-cancer agents: an underestimated truth. *Biomed Pharmacother*. 2019. <https://doi.org/10.1016/j.biopha.2018.12.119>.
- Kloskowski T, Szeliski K, Fekner Z, Rasmus M, Dąbrowski P, Wolska A, et al. Ciprofloxacin and levofloxacin as potential drugs in genitourinary cancer treatment—the effect of dose-response on 2D and 3D cell cultures. *Int J Mol Sci*. 2021. <https://doi.org/10.3390/ijms222111970>.
- Chrzanowska A, Olejarz W, Kubiak-Tomaszewska G, Ciechanowicz AK, Struga M. The effect of fatty acids on ciprofloxacin cytotoxic activity in prostate cancer cell lines—does lipid component enhance anticancer ciprofloxacin potential? *Cancers*. 2022. <https://doi.org/10.3390/cancers14020409>.
- Gupta P, Gao H-L, Ashar YV, Karadkhelkar NM, Yoganathan S, Chen Z-S. Ciprofloxacin enhances the chemosensitivity of cancer cells to ABCB1 substrates. *Int J Mol Sci*. 2019. <https://doi.org/10.3390/ijms20020268>.
- Pinto AC, Moreira JN, Simões S. Ciprofloxacin sensitizes hormone-refractory prostate cancer cell lines to doxorubicin and docetaxel treatment on a schedule-dependent manner. *Cancer Chemother Pharmacol*. 2009. <https://doi.org/10.1007/s00280-008-0892-6>.
- Park MS, Okochi H, Benet LZ. Is ciprofloxacin a substrate of P-glycoprotein? *Arch Drug Inf*. 2011. <https://doi.org/10.1111/j.1753-5174.2010.00032.x>.
- David-Beabes GL, Overman MJ, Petrofski JA, Campbell PA, de Marzo AM, Nelson WG. Doxorubicin-resistant variants of human prostate cancer cell lines DU 145, PC-3, PPC-1, and TSU-PR1: characterization of biochemical determinants of antineoplastic drug sensitivity. *Int J Oncol*. 2000. <https://doi.org/10.3892/ijo.17.6.1077>.
- Langdon SP. *Cancer cell culture*. Totawa: Humana Press Inc; 2010.
- Wang W, Wang L, Mizokami A, Shi J, Zou C, Dai J, et al. Down-regulation of E-cadherin enhances prostate cancer chemoresistance via Notch signaling. *Chin J Cancer*. 2017. <https://doi.org/10.1186/s40880-017-0203-x>.
- Munshi A, Hobbs M, Meyn RE. *Clonogenic cell survival assay*. Totawa: Humana Press Inc; 2005. <https://doi.org/10.1385/1-59259-869-2:021>.
- Aldaghi SA, Jalal R. Concentration-dependent dual effects of ciprofloxacin on SB-590885-resistant BRAFV600E A375 melanoma cells. *Chem Res Toxicol*. 2019. <https://doi.org/10.1021/acs.chemrestox.8b00335>.
- Li Y, Wang M, Zhi P, You J, Gao J-Q. Metformin synergistically suppress tumor growth with doxorubicin and reverse drug resistance by inhibiting the expression and function of P-glycoprotein in MCF7/ADR cells and xenograft models. *Oncotarget*. 2018. <https://doi.org/10.18632/oncotarget.23187>.
- Ciarimboli G. Introduction to the cellular transport of organic cations. In: Ciarimboli G, Gautron S, Schlatter E, editors. *Organic cation transporters*. Cham: Springer; 2016. [https://doi.org/10.1007/978-3-319-23793-0\\_1](https://doi.org/10.1007/978-3-319-23793-0_1).
- Zupkó I, Molnár J, Réthy B, Minorics R, Frank É, Wölfling J, et al. Anticancer and multidrug resistance-reversal effects of solanidine analogs synthesized from pregnadienolone acetate. *Molecules*. 2014. <https://doi.org/10.3390/molecules19022061>.
- Sims JT, Ganguly SS, Bennett H, Friend JW, Tepe J, Plattner R. Imatinib reverses doxorubicin resistance by affecting activation of STAT3-dependent NF-κB and HSP27/p38/AKT pathways and by inhibiting ABCB1. *PLoS ONE*. 2013. <https://doi.org/10.1371/journal.pone.0055509>.

29. Boesch M, Wolf D, Sopper S. Optimized stem cell detection using the DyeCycle-triggered side population phenotype. *Stem Cells Int*. 2016. <https://doi.org/10.1155/2016/1652389>.
30. Jouan E, Le Vee M, Denizot C, Da Violante G, Fardel O. The mitochondrial fluorescent dye rhodamine 123 is a high-affinity substrate for organic cation transporters (OCT s) 1 and 2. *Fundam Clin Pharmacol*. 2014. <https://doi.org/10.1111/j.1472-8206.2012.01071.x>.
31. Marquez B, Amey G, Vallet CM, Tulkens PM, Poirel HA, Van Bambeke F. Characterization of Abcc4 gene amplification in stepwise-selected mouse J774 macrophages resistant to the topoisomerase II inhibitor ciprofloxacin. *PLoS ONE*. 2011. <https://doi.org/10.1371/journal.pone.0028368>.
32. Wang D, Wang J, Zhang J, Yi X, Piao J, Li L, et al. Decrease of ABCB1 protein expression and increase of G1 phase arrest induced by oleanolic acid in human multidrug-resistant cancer cells. *Exp Ther Med*. 2021. <https://doi.org/10.3892/etm.2021.10167>.
33. Bray J, Sludden J, Griffin M, Cole M, Verrill M, Jamieson D, et al. Influence of pharmacogenetics on response and toxicity in breast cancer patients treated with doxorubicin and cyclophosphamide. *Br J Cancer*. 2010. <https://doi.org/10.1038/sj.bjc.6605587>.
34. Li Z, Chen C, Chen L, Hu D, Yang X, Zhuo W, et al. STAT5a confers doxorubicin resistance to breast cancer by regulating ABCB1. *Front Oncol*. 2021. <https://doi.org/10.3389/fonc.2021.697950>.
35. Phiboonchaiyanan PP, Kiratipaiboon C, Chanvorachote P. Ciprofloxacin mediates cancer stem cell phenotypes in lung cancer cells through caveolin-1-dependent mechanism. *Chem Biol Interact*. 2016. <https://doi.org/10.1016/j.cbi.2016.03.005>.
36. Lin M-C, Huang M-J, Liu C-H, Yang T-L, Huang M-C. GALNT2 enhances migration and invasion of oral squamous cell carcinoma by regulating EGFR glycosylation and activity. *Oral Oncol*. 2014. <https://doi.org/10.1016/j.oraloncology.2014.02.003>.
37. Heger JI, Froehlich K, Pastuschek J, Schmidt A, Baer C, Mrowka R, et al. Human serum alters cell culture behavior and improves spheroid formation in comparison to fetal bovine serum. *Exp Cell Res*. 2018. <https://doi.org/10.1016/j.yexcr.2018.02.017>.
38. Takeda N, Kondo M, Ito S, Ito Y, Shimokata K, Kume H. Role of RhoA inactivation in reduced cell proliferation of human airway smooth muscle by simvastatin. *Am J Respir Cell Mol Biol*. 2006. <https://doi.org/10.1165/rcmb.2006-0034OC>.
39. Schinkel AH, Jonker JW. Mammalian drug efflux transporters of the ATP binding cassette (ABC) family: an overview. *Adv Drug Deliv Rev*. 2012. <https://doi.org/10.1016/j.addr.2012.09.027>.
40. Thiery JP, Acloque H, Huang RY, Nieto MA. Epithelial–mesenchymal transitions in development and disease. *Cell*. 2009. <https://doi.org/10.1016/j.cell.2009.11.007>.
41. Shankaranarayanan JS, Kanwar JR, Al-Juhaishi AJA, Kanwar RK. Doxorubicin conjugated to immunomodulatory anticancer lactoferrin displays improved cytotoxicity overcoming prostate cancer chemo resistance and inhibits tumour development in TRAMP mice. *Sci Rep*. 2016. <https://doi.org/10.1038/srep32062>.
42. Amend SR, Torga G, Lin KC, Kostecka LG, de Marzo A, Austin RH, et al. Polyploid giant cancer cells: unrecognized actuators of tumorigenesis, metastasis, and resistance. *Prostate*. 2019. <https://doi.org/10.1002/pros.23877>.
43. Pienta KJ, Hammarlund EU, Axelrod R, Brown JS, Amend SR. Poly-aneuploid cancer cells promote evolvability, generating lethal cancer. *Evol Appl*. 2020. <https://doi.org/10.1111/eva.12929>.
44. Herbein G, Nehme Z. Polyploid giant cancer cells, a hallmark of oncoviruses and a new therapeutic challenge. *Front Oncol*. 2020. <https://doi.org/10.3389/fonc.2020.567116>.
45. Mirzayans R, Andrais B, Murray D. Roles of polyploid/multi-nucleated giant cancer cells in metastasis and disease relapse following anticancer treatment. *Cancers*. 2018. <https://doi.org/10.3390/cancers10040118>.
46. Song Y, Zhao Y, Deng Z, Zhao R, Huang Q. Stress-induced polyploid giant cancer cells: unique way of formation and non-negligible characteristics. *Front Oncol*. 2021. <https://doi.org/10.3389/fonc.2021.724781>.
47. Gupta SK, Singh P, Ali V, Verma M. Role of membrane-embedded drug efflux ABC transporters in the cancer chemotherapy. *Oncol Rev*. 2020. <https://doi.org/10.4081/oncol.2020.448>.
48. Zhou Y, Tozzi F, Chen J, Fan F, Xia L, Wang J, et al. Intracellular ATP levels are a pivotal determinant of chemoresistance in colon cancer cells. *Cancer Res*. 2012. <https://doi.org/10.1158/0008-5472.CAN-11-1674>.
49. Koziel R, Zabłocki K, Duszyński J. Calcium signals are affected by ciprofloxacin as a consequence of reduction of mitochondrial DNA content in Jurkat cells. *Antimicrob Agents Chemother*. 2006. <https://doi.org/10.1128/AAC.50.5.1664-1671.2006>.
50. Montani M, Herrmanns T, Müntener M, Wild P, Sulser T, Kristiansen G. Multidrug resistance protein 4 (MRP4) expression in prostate cancer is associated with androgen signaling and decreases with tumor progression. *Virchows Arch*. 2013. <https://doi.org/10.1007/s00428-013-1429-x>.
51. Davis R, Markham A, Balfour JA. Ciprofloxacin. *Drugs*. 1996. <https://doi.org/10.2165/00003495-199651060-00010>.
52. Boya P, Andreau K, Poncet D, Zamzami N, Perfettini J-L, Metivier D, et al. Lysosomal membrane permeabilization induces cell death in a mitochondrion-dependent fashion. *J Exp Med*. 2003. <https://doi.org/10.1084/jem.20021952>.
53. Vallet CM, Marquez B, Ngabirano E, Lemaire S, Mingeot-Leclercq M-P, Tulkens PM, et al. Cellular accumulation of fluoroquinolones is not predictive of their intracellular activity: studies with gemifloxacin, moxifloxacin and ciprofloxacin in a pharmacokinetic/pharmacodynamic model of uninfected and infected macrophages. *Int J Antimicrob Agents*. 2011. <https://doi.org/10.1016/j.ijantimicag.2011.05.011>.
54. Calcagno AM, Fostel JM, To KK, Salcido CD, Martin SE, Chewing KJ, et al. Single-step doxorubicin-selected cancer cells overexpress the ABCG2 drug transporter through epigenetic changes. *Br J Cancer*. 2008. <https://doi.org/10.1038/sj.bjc.6604334>.
55. Ware JH, Zhou Z, Guan J, Kennedy AR, Kopelovich L. Establishment of human cancer cell clones with different characteristics: a model for screening chemopreventive agents. *Anticancer Res*. 2007;27:1–16.
56. Jeon JH, Kim DK, Shin Y, Kim HY, Song B, Lee EY, et al. Migration and invasion of drug-resistant lung adenocarcinoma cells are dependent on mitochondrial activity. *Exp Mol Med*. 2016. <https://doi.org/10.1038/emm.2016.129>.
57. Friedrich J, Ebner R, Kunz-Schughart LA. Experimental anti-tumor therapy in 3-D: spheroids—old hat or new challenge? *Int J Radiat Biol*. 2007. <https://doi.org/10.1080/09553000701727531>.
58. Shah A, Lettieri J, Nix D, Wilton J, Heller A. Pharmacokinetics of high-dose intravenous ciprofloxacin in young and elderly and in male and female subjects. *Antimicrob Agents Chemother*. 1995. <https://doi.org/10.1128/AAC.39.4.1003>.
59. Segev S, Yaniv I, Haverstock D, Reinhart H. Safety of long-term therapy with ciprofloxacin: data analysis of controlled clinical trials and review. *Clin Infect Dis*. 1999. <https://doi.org/10.1086/515132>.

60. Gerding DN, Hitt JA. Tissue penetration of the new quinolones in humans. *Rev Infect Dis*. 1989. [https://doi.org/10.1093/clinids/11.Supplement\\_5.S1046](https://doi.org/10.1093/clinids/11.Supplement_5.S1046).
61. Naber KG, Sörgel F, Kees F, Jaehde U, Schumacher H. Brief report: pharmacokinetics of ciprofloxacin in young (healthy volunteers) and elderly patients, and concentrations in prostatic fluid, seminal fluid, and prostatic adenoma tissue following intravenous administration. *Am J Med*. 1989. [https://doi.org/10.1016/0002-9343\(89\)90023-5](https://doi.org/10.1016/0002-9343(89)90023-5).
62. Thakur A. Nano therapeutic approaches to combat progression of metastatic prostate cancer. *Adv Cancer Biol Metastasis*. 2021. <https://doi.org/10.1016/j.adcanc.2021.100009>.

**Publisher's Note** Springer Nature remains neutral with regard to jurisdictional claims in published maps and institutional affiliations.

Springer Nature or its licensor holds exclusive rights to this article under a publishing agreement with the author(s) or other rightsholder(s); author self-archiving of the accepted manuscript version of this article is solely governed by the terms of such publishing agreement and applicable law.